Exploring dissolved organic carbon cycling at the stream-groundwater interface across a third-order, lowland stream network

Sydney S. Ruhala[1], Jay P. Zarnetske[1*], David T. Long[1], Joseph A. Lee-Cullin[1], Stephen Plont[1], and Evan R. Wiewiora[1]

[1] *Department of Earth and Environmental Sciences, Michigan State University, East Lansing, Michigan, USA*

Keywords: DOC; stream-groundwater interactions; network scale; streams; carbon cycling.

[*] Corresponding Author. Department of Earth and Environmental Sciences, Michigan State University, 288 Farm Lane, Natural Sciences Building Room 207, East Lansing, Michigan, 48824, USA. *Email Address:* jpz@msu.edu (J.P. Zarnetske)

Abstract

The stream-groundwater interface (SGI) is thought to be an important location within stream networks for dissolved organic carbon (DOC) processing (e.g., degradation, removal), since it is considered a hotspot for microbial activity and biogeochemical reactions. This research assessed DOC cycling at the SGI across a third-order, lowland watershed in Michigan, USA. Since this work represents one of the first such assessments done at the network scale, we also summarized a systematic approach developed for data analysis of SGI porewaters, which may help guide future, network-wide DOC studies of the SGI. Chloride and temperature were used as natural tracers to determine the extent to which hydrological processes versus biogeochemical reactions influence DOC cycling at the SGI. Results show that there is no strong pattern of DOC removal within the SGI at the stream network scale. Instead, the trends in DOC quantity and quality suggest that the SGI system is more complex at local scales, which obscures its functioning at the network scale. For example, the mechanical mixing of ground and stream surface waters appears to explain the observed changes in DOC concentrations at some sites, while, biotic reactions, including aerobic microbial respiration, appear to influence DOC concentrations at other sites. Additionally, by sampling at the network scale, we were able to produce some of the first empirical SGI data that is compatible with recently developed process-based, network-scale, SGI models. The data indicate that these process-based models are not likely to accurately represent SGI exchange of the lowland, groundwater discharge-dominated stream in this study. Lastly, we were able to start to examine how DOC cycling at the SGI varies across the stream network and evaluate this within the frameworks of other stream network conceptual models for biogeochemistry. For instance, results show that sites with DOC removal at the SGI did not correlate with stream order or changes in local physical SGI flow patterns (i.e., streambed

upwelling or downwelling), bringing into question the utility of some stream carbon conceptual models (e.g., River Continuum Concept) for guiding SGI carbon biogeochemistry research.

Introduction

The zone beneath and alongside of the stream where stream water – groundwater interactions occur is thought to be an important location within stream networks for dissolved organic carbon (DOC) processing (e.g., degradation, removal). This is because the stream – groundwater interface (SGI) is considered a hotspot for microbial activity and biogeochemical reactions (Storey et al. 1999; Baker et al. 1999; Fischer et al. 2005; Battin et al. 2009; Zarnetske et al. 2011a). The hotspot arises as a result of the mixing of stream water and groundwater, which creates a transitional zone in the streambed sediments, promoting diverse microbial communities, metabolic pathways, and chemical reactions (Valett et al. 1996; Hedin et al. 1998; Findlay and Sobczak 2000; Nogaro et al. 2013; Boano et al. 2014). In addition, water residence times can increase at the SGI due to slow porewater transport, creating a longer exposure time of stream-borne DOC to microbial processing (Battin et al. 2008; Harvey et al. 2013; Boano et al. 2014).

Considering the documented reactivity of the SGI, it would be expected that the processes influencing DOC at the SGI would predominately result in the transformation and removal of DOC. Indeed, mesocosm and in-stream, reach-scale studies have shown decreased DOC concentrations along flowpaths through the SGI (Findlay et al. 1993; Findlay and Sobczak 1996; Schindler and Krabbenhoft 1998; Sobczak and Findlay 2002; Zarnetske et al. 2011b). These observations indicate that the SGI may be an important sink for DOC in stream networks. However, few studies have assessed DOC cycling at the SGI at the network scale (i.e., across an

entire watershed), and those that have, relied on mathematical models and upscaling rather than empirical field data (e.g., Wondzell 2011; Boano et al. 2014; Kiel and Cardenas 2014; Gomez-Velez and Harvey 2014). Further, few studies have thoroughly characterized changes in DOC quality (i.e., molecular characteristics, composition), in addition to DOC quantity (i.e., concentration), at any scale within the SGI (Findlay and Sobczak 1996). DOC qualities are critical variables to include in stream carbon studies since the qualities of DOC can change independently of DOC concentration (Lutz et al. 2012), and ultimately, impact DOC bioavailability and reactivity (i.e., lability). Thus, the quality of DOC is key to revealing the effects of DOC on downstream ecosystems and water quality (Fellman et al. 2010; Cory et al. 2011). Lastly, there are also seminal stream ecology and biogeochemistry concepts that relate changes in the surface water fate and transport of DOC to specific locations in a stream network, yet this has not been explored at the SGI (e.g., River Continuum Concept, Vannote et al. 1980; Shunt-Pulse Concept, Raymond et al. 2016). Thus, there is clearly a need for field studies to evaluate DOC quantity and quality and associated biogeochemical conditions at the network scale to support both the numerical modeling and ecological conceptual modelling efforts.

Here, we explore DOC cycling at the SGI in the Augusta Creek watershed in southwestern Michigan, USA (42°21'12"N, 85°21'14"W), which is a third-order, lowland stream network. To the best of our knowledge, this work represents the first network-scale sampling efforts of DOC at the SGI. Because there is a lack of previous work at this scale, there is no well-established approach for working at this scale to capture and analyze trends in DOC quantity and quality in the SGI. Therefore, in an effort to help develop a systematic approach to conduct investigations of the SGI at larger scales, we also summarize our procedure and lessons learned in working at these larger scales.

Research Questions and Hypothesis

The questions addressed in this study are: 1) is there evidence of DOC removal at the SGI across the stream network, 2) what processes (i.e., abiotic or biotic) are influencing DOC concentrations at the SGI, and 3) how consistent is the evidence for removal and types of processes occurring at the SGI across a site and the entire stream network?

There are multiple abiotic and biotic processes that affect the fate of DOC in the SGI. An abiotic process known to influence the cycling of DOC is sorption to sediment, which can account for removal of DOC in the SGI (McDowell 1985; Fiebig and Lock 1991; Findlay and Sobczak 1996). However, the extent of sorption and thus, removal of DOC is limited by the number of binding sites in the SGI. Once the sites are filled, DOC concentrations in the SGI will typically equilibrate with concentrations in upwelling or downwelling porewaters (e.g., Day et al. 1994; Kaplan and Newbold 2000). Therefore, if sorption was the only process influencing DOC in the SGI, then DOC concentrations would no longer show evidence of removal once the binding sites were filled (e.g., Dahm 1981; Fiebig 1995). For ongoing removal of DOC via sorption, binding sites would need to be regenerated. A potential mechanism for regeneration is the removal of previously sorbed DOC via microbial degradation (e.g., Findlay and Sobczak 1996; Kaplan and Newbold 2000). Considering this, sorption might play a key role in facilitating microbial degradation of DOC at the SGI. For example, sorption to the sediments would allow for more interaction time between DOC and microbes. In addition, microbes have long been known to sorb to sediments, creating biofilms (e.g., Marshall 1980; Wilkinson et al. 1995; Jamieson et al. 2005), which can remove adsorbed DOC, via diffusion into the biofilm, where DOC is then consumed via biological uptake (Kaplan and Newbold 2000). Thus, even though an

114 abiotic process such as sorption may sequester DOC, the ultimate process removing DOC at the
115 SGI is likely a biological process.

116 Microbial metabolism (i.e., consumption of DOC for energy production) is a biotic
117 process previously shown to remove DOC at the SGI in small-scale studies (e.g., Findlay and
118 Sobczak 1993). The metabolism of DOC results in transformations to the chemical structure and
119 reactivity of DOC (e.g., aromaticity, molecular weight), which then alters the fraction of labile
120 (more bioavailable) and recalcitrant (less bioavailable) DOC pools. Since microbes preferentially
121 consume labile DOC along flowpaths, a more recalcitrant pool of DOC is likely transported
122 downstream (Fellman et al. 2010; Cory et al. 2011). For example, microbially processed DOC
123 tends to have a lower molecular weight and be less aromatic than "fresh", terrestrially-derived
124 DOC from vascular plant sources (McKnight et al., 2001; McDonald et al., 2004; Fellman et al.,
125 2010). Therefore, the chemical structure and composition of DOC can be used to help identify if
126 microbial processes have transformed or removed DOC at the SGI. Considering that the
127 structural complexity of DOC makes it difficult to study DOC composition (Cory et al. 2011),
128 optical properties of DOC, determined via ultraviolet-visible (UV-VIS) absorbance
129 spectroscopy, can be used to assess the chemical structure and thus the quality of DOC (e.g.,
130 Weishaar et al. 2003; Cory et al. 2011; Jollymore et al. 2012; Creed et al. 2015; Ruhala and
131 Zarnetske 2017), instead of complex analytical methods (e.g., mass spectrometry). For instance,
132 specific ultraviolet absorbance at a wavelength (λ) of 254 nm (i.e., $SUVA_{254}$) can be used to infer
133 DOC aromaticity since electron structures associated with aromatic carbon molecules absorb
134 energy at this wavelength, while other structures do not (Weishaar et al. 2003). Similarly, a
135 spectral slope ratio (i.e., S_R) can be used to infer DOC molecular weight.

Overall, we hypothesize that, for individual SGI sites as well as across the stream network, biotic processes, rather than abiotic processes, are predominantly transforming DOC at the SGI and that the dominant biotic process is aerobic microbial respiration (i.e., consumption of DOC and O_2 for metabolism and release of CO_2). To test the hypothesis, we conducted synoptic sampling of the SGI across the Augusta Creek watershed over an 8-day period in August 2016. If the hypothesis is true, then we expect to not only see DOC concentrations consistently decrease in the SGI, but that there are also changes in DOC quality that are consistent with microbial processes as evidenced by changes in DOC chemical structure (as shifts in $SUVA_{254}$ and S_R) and DOC – DO metabolism relationships.

Background

Field Site Description

The Augusta Creek watershed is located in southwestern Michigan, USA and is part of the larger Kalamazoo River watershed (Fig. 1). This watershed was selected as the field site because Augusta Creek is a historically important stream for biogeochemical and ecological research (e.g., it was an original River Continuum Concept and Natural Flow Regime site; Vannote et al. 1980; Poff et al. 1997), has a long-term and active United States Geological Survey (USGS) gaging station (04105700), and is associated with the Kellogg Biological Station Long-Term Ecological Research site, which helps provide easy access through roadways, university lands, and land use partnerships. The watershed was heavily influenced by glacial activity with the most recent being the late Pleistocene Epoch (Dunbar 1962). As a result, the watershed is underlain by glacial deposits consisting of mixtures of gravel, sand, silt, and clay, varying in thickness from 40 to 120 m (FTWRC 2011).

159 Augusta Creek is a third-order, lowland watershed draining 98 km^2 (Fig. 1; Strahler
160 1957). Most of the tributaries originate in groundwater-fed lakes and low-lying wetlands (Manny
161 and Wetzel 1973; FTWRC 2011) and most sections of the stream network gain flow via
162 groundwater discharge. The three dominant land cover types are 1) 47% is agriculture (crops and
163 pastures), 2) 23% is upland forest (mainly deciduous), and 3) 20% is wetland/marsh complexes
164 (FTWRC 2011). The mean annual precipitation is 1005 mm, and the total precipitation in 2016
165 was 975 mm (NCDC 2013; KBS-LTER Dataset KBS002). Soils are typically sandy to loamy in
166 uplands, with organic (muck) soils in the riparian wetlands, and patches of muck along the
167 stream channel (FTWRC 2011). Soil infiltration rates throughout the watershed range from 12.7
168 to 25.4 mm/h and the mean stream slope is approximately 2.03 m/km (Manny and Wetzel 1973;
169 FTWRC 2011).
170 In general, Augusta Creek is considered a hard water stream with a total hardness of
171 about 280 mg/L (Mahan and Cummins 1974; King 1978). Alkalinity typically ranges from 160
172 to 210 mg/L as $CaCO_3$, while pH ranges from 7.5 to 8.7 (Manny and Wetzel 1973; Mahan and
173 Cummins 1974; King 1978). Calcite ($CaCO_3$) precipitates are often found on stones on the
174 stream bottom. Additionally, marl ($CaCO_3$-rich) and clay lenses are found throughout the
175 streambed sediments. Sampling of Augusta Creek from 1997-2015 has shown that stream DOC
176 concentrations typically range from 2 to 12 mg/L (Hamilton SK, personal communication, 2017)
177 *Hydrology*
178 Augusta Creek exhibits a discharge flow regime characterized as having minimal within-
179 and among-year variation (Url and Hart 1992; Poff et al. 1997). Based on recent and historical
180 discharge measurements collected at the USGS gaging station (04105700) located on the lower
181 main stem above the Kalamazoo River confluence (Fig. 1), the average range in discharge for

Augusta Creek during the month of August is 0.54 to 2.06 m^3/s (based on daily mean values from August 2011 to August 2016; USGS 2017, Station 04105700). Our synoptic sampling campaign took place from August 15 – August 22, 2016, during which the average discharge was 1.35 m^3/sec, higher than the previous 5-year average of 1.08 m^3/sec for the month of August (USGS 2017, Station 04105700). During the sampling period, discharge varied some from 1.08 to 3.65 m^3/sec (Fig. 2), which equates to a stage change of 0.36 to 0.73 m at the confined channel gaging station, but we observed that this only equated to millimeters to centimeters of potential stage change across most reaches and sampling sites of the stream network.

Methods and Materials

The systematic approach that evolved during the course of this study to test the hypothesis is summarized in Fig. 3. We highlight the key steps within this approach to capture SGI biogeochemistry at many sites across our study watershed and subsequently how to analyze the data that accounts for various controls on DOC observations. Briefly, following the development of a specific hypothesis to address the research questions (see subsection *Research Questions and Hypothesis)*, we designed a sampling scheme that stratified sites across steam orders to evenly represent the total stream network length (i.e., most sites in first-order reaches that represent the majority of stream network length and least sites in third-order reaches). At each site, we collected an appropriate range of physical and chemical measurements needed for data analysis. Data collection efforts are balanced by a trade-off between the amount of time spent at one site versus the number of sites visited. Data collection included measurement of natural ionic and heat tracers, such as dissolved Cl^- and temperature. These tracers are key to characterizing physical mixing of surface and groundwater end-members within the SGI. Determining this

mixing is necessary for examining porewater profiles and mixing models to identify the types of processes (e.g., physical dilution vs. biological uptake) driving changes in DOC at the SGI, and therefore, address our specific hypothesis. Overall, the average time spent at one sampling site was 1.5 h. Finally, due to the large size and complexity of the dataset, another key to our approach was to identify DOC and natural tracer patterns at different scales including, network, sub-network (stream order) and individual sample site scales. This general approach (Fig. 3) will help guide future SGI biogeochemical investigations that require network-scale observations, especially where groundwater discharge (upwelling) occurs throughout much of the stream network.

Sample Collection

There were 39 sites across the watershed where SGI porewater, stream surface water and groundwater samples were collected for analysis (Fig. 1). These sites were selected to stratify sampling by stream order and to capture the range of variability in land use/cover across the Augusta Creek watershed (see Supplemental Information, Fig. S1), while recognizing site and property access limitations. Porewater samples were collected using a custom built MINIPOINT porewater sampler, for the temporary installation of nested piezometers (e.g., Duff et al. 1998; Fig. 4). The MINIPOINT consists of six 50 cm-long by 0.5 cm-diameter piezometers arranged in a 10 cm-diameter circular array (Fig. 4a). The piezometers are adjustable allowing for high-resolution, vertical porewater profile sampling that is minimally disruptive to the sediment column as well as the ambient chemical and biological processes occurring at the SGI (Duff et al. 1998). For this study, a single MINIPOINT sampler was deployed at each site with the 6 piezometers vertically staggered at streambed sediment depths of 2.5, 5.0, 7.5, 10, 15, and 20 cm. The placement of the MINIPOINT in the stream channel was largely dependent on finding areas

where the sediment type was conducive to the piezometer, which means samples were not collected in cobble- or clay-rich sediments that preclude installation of the sampler. This reasoning is also why we selected 20 cm as the deepest sampling depth in the SGI since interference from buried cobbles and unconducive sediment types increased at greater depths. Porewater samples were simultaneously extracted from all 6 SGI depths using a multi-channel peristaltic pump (i.e., Cole Palmer Masterflex L/S Peristaltic Pump) set at a low flow rate (i.e., 1.5-2.5 mL min^{-1}) to minimize or eliminate the disturbances to the natural groundwater flow field (Fig. 4b; Harvey and Fuller 1998). Approximately 60 mL of sample per SGI depth was pumped into a 100 mL-BD syringe that was connected with the peristaltic pump and corresponding piezometer using Tygon tubing with a 1.59 mm-inner diameter and Masterflex Norprene Food Tubing with a 1.59 mm-inner diameter.

A stream surface water sample was collected at each site at least 5 cm below the stream free-surface, using a 100 mL-BD syringe. In addition, a drive-point well installed to a depth of 60 cm below the stream-sediment interface was used to collect a porewater sample that is representative of site groundwater. Prior to groundwater sampling, the drive-point well was purged until the water became clear, allowed to equilibrate for a minimum of 45 min and then a vertical head gradient (VHG) was measured. A positive VHG indicates upwelling groundwater, while a negative VHG indicates downwelling stream water. Once the VHG was determined, the groundwater sample was slowly drawn into a 100 mL-BD syringe, which was connected to a 6.35 mm-inner diameter polyethylene tube that extended down the drive-point well to a streambed depth of 60 cm. All samples (i.e., stream water, groundwater, and porewater) were filtered in the field, first through a glass microfiber filter (i.e., Whatman GF/F 25 mm-diameter filters, 0.7 µm pore size) and then through a cellulose acetate filter (i.e., Sartorius Stedim, 0.2 µm

pore size) directly into two, 30 mL, acid-washed, HDPE amber bottles (to prevent photodegradation), one of which was used for DOC analysis and the other for analysis of various ions. The bottles were kept on ice as required by US EPA method 415.3 (Potter and Wimsatt 2003) until return to the laboratory, where the samples were stored in the dark, at 4 °C until analyzed.

Dissolved oxygen (DO) was measured at each site using a fiber-optic oxygen meter (Pyro Science FireStingO_2, Pyro Science, Aachen, Germany). Dissolved oxygen readings were made at all SGI porewater depths, stream water, and groundwater using sealed flow-through cells (Pyro Science Flow-Through Cells, Pyro Science, Aachen Germany) that were connected to each MINIPOINT piezometer. Temperature was measured at each SGI depth using a ThermoWorks Type T Heavy-Duty Temperature Probe with 6.35 mm-diameter (ThermoWorks, Utah, USA), while stream and groundwater temperature was measured using the fiber-optic oxygen meter temperature probe.

Analytical Methods

DOC concentrations (measured as Non-Purgeable Organic Carbon, NPOC) were analyzed via high-temperature combustion using a Shimadzu TOC-L Analyzer (Shimadzu Scientific Instruments, Kyoto, Japan). In addition, a Dionex ICS-2100 ion chromatograph (Thermo Fisher Scientific, Massachusetts, USA) was used to analyze the samples for NO_3^-, Cl^-, and SO_4^{2-} concentrations. Ion analysis was completed using an AS19 Dionex IonPac column (2 x 250 mm) with a potassium hydroxide (KOH) eluent generator and a 0.25 mL min^{-1} flow rate. Optically-derived DOC quality indicators were determined from absorbance data collected on a Shimadzu dual-beam UV 1800 spectrophotometer (Shimadzu Scientific Instruments, Kyoto, Japan). Absorbance readings were taken over the entire UV-VIS range from 220 to 800 nm using

semi-micro, BrandTech cuvettes with a 1-cm path length and EPure water (i.e., 18 ohm, Barnstead EPure system) as the blank. Each cuvette was triplicate rinsed with EPure water between samples.

In this study, $SUVA_{254}$ was used to infer DOC aromaticity. $SUVA_{254}$ was obtained by measuring the sample's absorbance at λ=254 nm and dividing by the DOC concentration of the sample (units are L/mg C/m). An increase in $SUVA_{254}$ values is associated with an increase in aromaticity (Weishaar et al. 2003). In addition, S_R was used as a proxy for molecular weight and was determined by taking the ratio of the slope of the 275-295 nm absorbance spectra over the slope of the 350-400 nm absorbance spectra. An increase in S_R values is associated with a decrease in DOC molecular weight.

For data visualization, vertical profiles were constructed of the optical properties and solute species (Fig. 4c). Profiles combined the stream water, porewater and groundwater samples at each site. See Supplemental Information (Fig. S2-S40) for the vertical porewater profiles of DOC concentration, DO, $SUVA_{254}$, S_R, NO_3^-, SO_4^{2-}, Cl^-, and temperature for the individual sites.

Results

General Concentrations

The mean DOC concentration in stream water collected from the 39 sampling sites was 8.84 mg/L with a median of 8.91 mg/L and a range of 5.31 to 13.63 mg/L. This is consistent with previous measurements of mean DOC concentrations for Augusta Creek, which ranged from 2 to 12 mg/L (Hamilton SK, personal communication, 2017). For groundwater, the mean DOC concentration sampled across the watershed was lower than that of stream water at 6.52 mg/L with a median value of 5.79 mg/L and ranged from 2.42 to 14.15 mg/L. For the SGI, which we

297 consider here to be between 2.5 and 20 cm depth below the streambed, the mean porewater
298 concentration was 6.46 mg/L with a median value of 6.22 mg/L and ranged from 1.35 to 17.04
299 mg/L, with the exception of Site F1, which had a peak DOC concentration of 38.46 mg/L and is
300 located immediately downstream of a large wetland complex (Fig. S1).

301 Stream water across Augusta Creek was well oxygenated with DO levels greater than
302 approximately 5 mg/L during the entire sampling campaign. The mean DO concentration in
303 stream water was 6.82 mg/L with a median value of 6.86 mg/L and a range of 4.91 to 9.32 mg/L.
304 For groundwater, the mean DO concentration was 3.15 mg/L with a median value of 1.85 mg/L
305 and ranged from 0.31 to 12.82 mg/L. For the SGI, the mean DO concentration was 1.75 mg/L
306 with a median value of 0.73 mg/L and ranged from 0.04 to 9.53 mg/L.

307 *Composite Vertical Porewater Profiles*

308 Individual vertical porewater profiles for the 39 sites were averaged to create composite
309 vertical porewater profiles for DOC, DO, $SUVA_{254}$, and S_R (Fig. 1; Fig. 5, graphs labeled "All
310 Sites"). In addition, composite vertical porewater profiles were created as a function of stream
311 order (Fig.1; Fig. 5). Using composite vertical porewater profiles was our first step in identifying
312 patterns in trends in DOC quantity and quality in the SGI at the network and sub-network (i.e.,
313 stream order) scales.

314 These composite vertical porewater profiles most commonly showed decreasing DOC
315 concentrations with depth through the SGI. This is seen in both the mean network profile (i.e., all
316 sites) and in the mean profiles for each stream order (Fig. 5a). Other trends observed were that
317 for third-order streams, DOC concentration increased between depths 7.5 and 10 cm and a slight
318 increase in DOC concentration was observed between depths 2.5 and 5 cm in the first-order
319 vertical profile (Fig. 5a).

Dissolved oxygen concentrations decreased with depth through the SGI in the mean network profile and in the mean profile for each stream order, typically becoming depleted with concentrations of 2 mg/L DO or less at deeper SGI depths (Fig. 5b). Groundwater measurements taken from 60 cm depth showed lower DO concentrations than stream water, but higher than the DO concentrations observed at 20 cm depth in the SGI in the composite profiles (Fig. 5b).

In terms of the optical properties, $SUVA_{254}$ generally decreased with depth at the SGI in the mean network profile and in the mean first-order and third-order profiles (Fig. 5c), but showed an increase in variability relative to stream and ground waters. There was also a small increase in $SUVA_{254}$ observed at intermediate SGI depths of about 7.5 to 10 cm in the second-order vertical profile (Fig. 5c). For S_R, an increase with depth was observed in all mean vertical porewater profiles (Fig. 5d). Overall, the greatest variability in DOC quantity and qualities consistently occurred in the SGI across the watershed.

Individual Site Vertical Porewater Profiles

Overall, the composite vertical porewater profiles for the network and each stream order show similar trends in DOC concentration, DOC quality parameters, and DO measurements. However, there were some key differences noted between individual sites that reflect the influence of the site variability in hydrological and biogeochemical parameters (see Supplemental Information, Fig. S2-S40). For example, the observed increase in $SUVA_{254}$ at intermediate SGI depths in the second-order vertical profile is predominantly the result of two sites (F2 and F4), which are adjacent to a large wetland complex that may provide an additional source of aromatic DOC to the SGI in that stream reach. Nonetheless, in looking at the variability of the vertical profiles of DOC concentration amongst the individual sites, we observed three dominant trends with depth – 1) no change, 2) continual decrease, and 3) "hook"

(Fig. 6). Five of the 39 sites showed no change in DOC concentration with depth at the SGI (Fig. 6a). At 26 sites, concentrations of DOC continually decreased with SGI depth (Fig. 6b.) and at 6 sites concentrations exhibited a "hook" shaped trend in which DOC concentrations decreased from shallow depths to a minimum value at some intermediate depth and then again increased at deeper depths through the SGI, toward groundwater conditions (Fig. 6c). There were 2 sites, F1 and G1, which did not fit any of these trends. Site F1 showed a significant peak in DOC concentration at intermediate SGI depths (see *General Concentrations)*, but again this site is influenced by a large wetland complex, which likely effects DOC conditions along the stream reach where the F sites are located. For Site G1 porewater samples were limited resulting in an incomplete vertical porewater profile, which prevented comparison to the representative trends (see Supplemental Information, Fig. S18). These three general profile trends indicate that numerous, possible physical, chemical or biological processes are influencing DOC concentration at the SGI of the watershed and that using single, mean values to identify processes at the network or sub-network scale for the development of subsequent SGI biogeochemical models may lead to some degree of error. Below we explore these potential processes that may explain these profile trends in DOC quantity and quality at the SGI by using the systematic processing approach shown in Fig. 3.

Discussion

The composite vertical porewater profiles (Fig. 5) for Augusta Creek in 2016 conformed to most previous SGI studies and our expectations of decreasing DOC and DO concentrations with depth at the SGI. Furthermore, concentrations in the SGI in the composite profiles were lower than that of either the overlying stream water or the underlying groundwater. Thus, simple mixing of

366 stream water and groundwater at the SGI alone cannot account for the observed decreases in
367 DOC and DO (e.g., Pinder and Jones 1969). Other processes must be occurring at the SGI to
368 account for the reduced DOC and DO concentrations.

369 The composite profiles showed decreasing $SUVA_{254}$ and increasing S_R with depth at the
370 SGI, indicating that DOC aromaticity and molecular weight decreased through the SGI
371 (Weishaar et al. 2003; Helms et al. 2008). These trends and those of DOC and DO
372 concentrations are consistent with what might be expected if microbially driven DOC
373 transformations were consuming DOC at the SGI. This supports our hypothesis that a biological
374 reaction, potentially, aerobic microbial respiration, is removing DOC at the SGI across the
375 watershed. This general pattern may further guide the development of a conceptual framework
376 for DOC processing in the SGI that will help refine existing models of DOC dynamics at the
377 watershed scale (e.g., McKnight et al. 2001; Fellman et al. 2010; Cory et al. 2011; Mann et al.
378 2012; Creed et al. 2015; Helton et al. 2015). However, as noted, at the individual site scale DOC
379 concentration patterns appear to be more variable and indicate distinct SGI processes.

380 In this study, we observed three different SGI trends that help determine the fate of DOC
381 at the SGI of this lowland, groundwater-dominated stream. For the sites that exhibit no change in
382 DOC concentration with depth, we cannot conclude that either abiotic or biotic processes are
383 influencing concentrations of DOC. The other two trends (i.e., decreasing DOC with depth and
384 the "hook" trend) are consistent with biotic removal. However, these two trends require further
385 analysis to confirm biotic removal, because the influence of mechanical, source water mixing on
386 these trends needs to be taken into account. For example, the sites showing a decrease in DOC
387 concentration with depth could simply result from the mixing of stream water and groundwater
388 that differ in DOC concentrations and not the result of biotic removal. Therefore, to determine

389 the extent to which mixing influences the trends at the SGI, we need to utilize additional data and
390 methods to deconvolve the effects of mixing versus biogeochemical processing. Here, we used a
391 binary mixing model to isolate the mixing effects as discussed below.
392 *Evaluating the Influence of Mixing on DOC Trends*
393 To identify the influence of source water mixing on the observed trends in the individual
394 site vertical porewater profiles (Fig. 3), we used naturally occurring chloride (Cl^-)
395 concentrations, as Cl^- is assumed to be conservative in most SGIs, to predict what the
396 concentration of DOC should be at each depth in the SGI. This can be accomplished assuming
397 one-dimensional (1D) vertical mixing of two end-member waters alone (Peters and Ratcliffe
398 1998). If predicted DOC concentrations and trends match observed DOC concentrations at a site,
399 then we can conclude that mixing is controlling the trends in DOC at the SGI, and therefore,
400 removal processes are not controlling the trends in DOC. If predicted and observed
401 concentrations of DOC do not agree, then DOC removal (or production) processes, most likely
402 biotic, must also be occurring in addition to some degree of mixing.
403 Chloride concentrations at depths of 2.5 and 20 cm were used as the end members in the
404 binary mixing model (Eq. 1) used to predict the degree of mixing. We selected 2.5 cm as the
405 shallow end-member instead of stream water, because although we had stream water Cl^-
406 concentrations, those stream water values could be more variable over shorter time scales than
407 the porewater values. Thus, the measured stream water values do not best define the shallow
408 porewater end-member. Further, to better define the deeper end-member we selected 20 cm
409 instead of groundwater (60 cm) due to the lack of vertical porewater samples taken between 20
410 cm and 60 cm. In addition, the major changes in DOC concentrations (e.g., the “hook” pattern)

411 consistently occurred between 2.5 and 20 cm across the watershed (Fig. 5). Consequently, the
412 binary mixing model used in this study is as follows:

$$\%E_{1,x} = \frac{[Cl^-]_x - [Cl^-]_{E_2}}{[Cl^-]_{E_1} - [Cl^-]_{E_2}} \times 100 \quad (1)$$

413 Where:

414 x = the depth of interest between 2.5 and 20 cm

415 $\%E_{1,x}$ = the percentage of the 2.5 cm end-member at depth x.

416 $[Cl^-]_x$ = the Cl^- concentration at the depth of interest

417 E_1 = Cl^- concentration at 2.5 cm depth for the site

418 E_2 = Cl^- concentration at 20 cm depth for the site

419

420 If SGI flow is 1D, then vertical mixing of the end-member waters can account for the
421 concentrations of Cl^- observed between 2.5 and 20 cm in the SGI, and the calculated percentage
422 of each end-member water present at every SGI depth will fall between 0 and 100% for that site.
423 If the percentages fall outside of that range, then the 1D vertical mixing of the end-member
424 waters alone cannot produce the observed Cl^- concentrations. For 15 of the 39 sites, the
425 percentage of each end-member water present at every depth in the SGI fell between 0 and 100%
426 (Table 1, sites in white; note that for Site R1 end-members of 2.5 and 10 cm were used since we
427 were not able to retrieve samples at depths greater than 10 cm; Fig. S35). Thus, for these 15 sites,
428 1D, vertical mixing of the end-members fully explains the Cl^- concentrations observed between
429 2.5 and 20 cm. For the other 24 sites, the percentages of each end-member water present at SGI
430 depths fell outside of the 0 to 100% range (Table 1, sites shaded in gray). Therefore, 1D vertical
431 mixing alone cannot explain the observed trends in concentrations of Cl^- at those 24 sites. This
432 might indicate that another water source, for example, from lateral flow coming into the profile

between 2.5 and 20 cm, is influencing the chemistry of water in the SGI at those 24 sites. Since, the chemistry of this other water source is not known, we selected to use only the 15 sites that can be constrained by the 1D vertical mixing assumptions in our predictive DOC mixing model analysis. For these 15 sites, we then predicted the concentration of DOC at all SGI depths based on the percentage of the end-member waters present at each depth as follows (Eq. 2):

$$[DOC]_x = \left[\%E_{1,x} \times \left([DOC]_{E_1} - [DOC]_{E_2} \right)\right] + [DOC]_{E_2} \quad (2)$$

Where:

$[DOC]_x$ = predicted concentration of DOC at depth of interest x between 2.5 and 20 cm

$\%E_{1,x}$ = the percentage of the 2.5 cm end-member at depth x

$[DOC]_{E1}$ = concentration of DOC at depth 2.5 cm at the site

$[DOC]_{E2}$ = concentration of DOC at depth 20 cm at the site

The predicted concentrations of DOC are what we would expect to see if the changes in DOC at the SGI were the result of mechanical, 1D vertical mixing with no additional abiotic or biotic reactions. See Supplemental Information to see the predicted DOC vertical profiles for each site.

We then compared the predicted DOC concentrations to the observed concentrations at each SGI depth for the 15 sites to assess the extent to which trends in DOC concentrations with depth were controlled by mixing versus other transformation processes (Fig. 3; Fig. 7). We considered that there was a difference between the predicted and observed DOC concentrations if the concentrations at two or more depths within the vertical profile varied by more than 10%. Based on this definition, 3 of the 15 sites exhibited no difference in predicted and observed DOC concentrations, indicating that changes in DOC at those 3 sites are controlled only by 1D vertical mixing between 2.5 and 20 cm, especially where there was strong groundwater discharge

455 (e.g., upwelling at Site O1; Fig. 7a; Table 1). Additionally, there were 4 out of the 15 sites that
456 showed more DOC with depth in the SGI than predicted by the mixing model (Fig. 7b; Table 1).
457 This suggests that in addition to vertical mixing, abiotic or biotic reactions at the SGI are
458 producing DOC or that there is a reservoir of organic carbon generating DOC in the streambed
459 sediment. For example, this could potentially be explained by microbial utilization and
460 decomposition of particulate organic carbon (POC), such as leaves and buried logs in the
461 streambed subsurface, which would result in the production of autochthonous (e.g., microbially-
462 derived) DOC (e.g., Stelzer et al. 2015). Out of the 15 sites there were 7 sites that showed clear
463 evidence of removal of DOC with depth in the SGI (i.e., less DOC with depth in the SGI that
464 predicted by the mixing model; Fig. 7c). Finally, the one remaining site, Site O2, did not show a
465 clear trend (Table 1). Having now identified the sites that show clear DOC transformation versus
466 only mechanical mixing effects, it is possible to apply additional methods to evaluate the DOC
467 removal mechanisms at the SGI (Fig. 3).
468
469 *Evaluating the DOC Removal Mechanism at the SGI*
470 Using the 7 SGI sites that showed clear evidence of DOC removal, we attempted to
471 assess if the removal was driven by a biotic process, specifically aerobic microbial respiration, as
472 originally hypothesized. We used "metabolism plots", based on methods from Findlay and
473 Sobczak (1996) and Battin (1999), to evaluate the role of aerobic respiration on DOC. In their
474 construction of the metabolism plots, stream DO concentration minus porewater DO
475 concentration was plotted against stream DOC concentration minus porewater DOC
476 concentration for a given site. The porewater values were obtained from a fixed depth at all of
477 their sites. If aerobic microbial respiration was the only transformation mechanism consuming

DOC over that range in depth, then the sample would plot on or along the 1:1 molar line (Fig. 8a). This assumes that for every 1 mole of carbon consumed, 1 mole of oxygen (O_2) is consumed, thus only accounting for minimal O_2 consumption since the ratio is not corrected for diffusion of O_2 (Findlay and Sobczak 1996). Samples that fall to the left of the 1:1 molar line indicate that for the given porewater sample, more DO was removed than what can be explained by DOC consumption, again assuming aerobic, microbial respiration. Samples that plot to the right of the 1:1 molar line indicate that for the given porewater sample, more DOC was removed than what can be explained by DO consumption alone (Fig. 8a).

Our metabolism plots were created using a modification of the technique by Findlay and Sobczak (1996) described above (Fig. 8). Firstly, we have additional depth and mixing data than they did, so we make no assumptions about the presence of a hyporheic zone, as they did, and we are simply exploring the SGI. Secondly, in looking at the high degree of variability seen in our high-resolution data (see Supplemental Information, Fig. S2-S40), using a single, fixed depth as they did for the calculations was not justifiable. Therefore, the change in concentration of DOC for our first metabolism plot (Fig. 8a) was calculated as the difference between the observed DOC concentration at 2.5 cm and the observed DOC concentration at the greatest depth between 2.5 and 20 cm that showed clear evidence of removal based on the corresponding profile for predicted DOC concentrations (see Table 1 for determined depth ranges; note the depth used varied by site). This approach is similar to that of Findlay and Sobczak (1996), but differs because 1) we consider the greatest depth exhibiting DOC concentration depletion, not a fixed depth and 2) we know that DOC has been depleted by processes other than dilution based on comparison to the predicted DOC profiles. Removing these assumptions from the metabolism

plot yields more confidence in its interpretation. Similarly, the change in concentration of DO was then calculated using the same depth range in the SGI for a given site (Table 1).

Overall, the metabolism plot based on corrected concentration differences show that the 7 sites clustered to the right of the 1:1 molar line, indicating that more DOC was removed in the SGI than can be explained by DO consumption via aerobic microbial respiration alone (Fig. 8a). However, while these 7 sites showed evidence of DOC removal at the SGI, some of the change in DOC concentration along the observed vertical profile did not show consistent DOC reduction between individual depths, therefore some of the DOC mass lost is not accounted for by using a two point difference calculation (Supplemental Information, Fig. S6, S7). We can capture more accurately the net DOC transformation by integrating the DOC loss between the predicted and observed DOC concentration profiles. Thus, allowing for a more precise estimate of actual DOC mass removal to use in the metabolism plot analysis of the 7 SGI sites (Table 1). The end result is an adjusted metabolism plot (Fig. 8b) that uses total integrated mass differences in DOC and DO over the depth profile, and is not limited by the assumptions of the concentration differences that can mask overall mass transformation (see Supplemental Information for a more complete explanation of determination of DOC and DO mass lost across the SGI).

The change in mass of DOC and DO (in μmol) for the 7 sites yields a metabolism plot (Fig. 8b) in which the sites still clustered to right of the 1:1 molar line, with the exception of one site. The observations clustered closer to the 1:1 molar line than when using the less conservative, concentration difference approach (Fig. 8a, b). Still, we can be confident that more DOC was removed at the SGI of these 6 sites than what can be explained by DO consumption alone (Fig. 8b). Based on these trends, aerobic microbial respiration is likely one of the reactions driving DOC removal at the SGI of these 6 sites as it is energetically the most preferential to

other respiration pathways (Baker et al., 1999). It is important to note that diffusion of O_2, while not likely in these SGI porewaters, is not accounted for using this method and therefore could partially explain the observed deviation to the right of 1:1 molar line in the adjusted metabolism plot (Findlay and Sobczak 1996; Fig. 8b). Additionally, DOC might provide electrons to other less energetically favorable terminal electron acceptors, such as nitrate and sulfate, at depths were DO is limiting aerobic respiration (Baker et al., 1999). These additional electron acceptor pathways may account for some of the "missing" DOC in our metabolism analysis. The single site that plots to the left of the 1:1 molar line is Site I2, which is one of the largest sections of the stream network - a third-order site located in the lower main stem above the Kalamazoo River confluence. Here, the metabolism plot shows that more DO is removed at the SGI at Site I2 than can be explained by DOC consumption via aerobic microbial respiration. A possible explanation is that DO could be used in microbial processing of buried POC in addition to DOC (Stelzer et al. 2015).

Finally, we questioned if changes in DOC and DO concentrations at the SGI may be dependent on flow direction of the water (i.e., upwelling or downwelling through the streambed). For example, upwelling water might bring in older, more recalcitrant DOC that would be harder to consume via biotic reactions than fresher, more labile DOC from the surface waters (e.g., Cory et al. 2011). Therefore, we used VHG data to group the 7 sites by flow direction. Out of the 7 sites, 2 were downwelling, 2 were upwelling, and 3 did not yield a distinct VHG. Therefore, there is limited data to assess the effect of flow direction, but the sites here show no pattern that would suggest flow direction influences the reactions removing DOC at the SGI (Fig. 8c).

Evaluating Variations in DOC Cycling across the Stream Network

We are able to start to assess the variability of DOC processing across a stream network in this study (e.g., varying transformation/removal mechanisms). As a first approximation of this variability, we might assume that a framework similar to the River Continuum Concept also applies to the SGI (Vannote et al. 1980) as stream water is the primary source of DOC to many SGIs. Thus, we predicted that more DOC processing, leading to removal, would occur in the headwater (lower order) streams than in the higher stream orders across the network. This is because changes in channel slope and streambed morphology tend to control rapid SGI exchange, specifically hyporheic exchange, in lower stream orders, whereas regional groundwater discharge and recharge control SGI exchange in higher (main stem) stream orders (e.g., Battin et al. 2008; Boano et al. 2014). In addition, subsurface flowpaths that feed higher stream orders also tend to have lower chemical variations due to longer residence times along subsurface flowpaths, which limits microbial reactivity (Battin et al. 2008; Harvey et al. 2013; Boano et al. 2014). The stream also becomes less directly connected to adjacent wetlands and the terrestrial landscape as stream order increases, thus reducing inputs of complex allochthonous DOC (e.g., terrestrial vascular-plant derived; Vannote et al. 1980). Furthermore, we predicted that more DOC transformations would occur at sites with downwelling water since upwelling groundwater may limit the extent of the SGI, resulting in a smaller region of stream-groundwater interactions, limiting processing of DOC at the SGI (e.g., Cardenas and Wilson 2007; Boano et al. 2009).

When we evaluate these predictions for DOC across the SGI, we see that the composite vertical porewater profiles showed consistent trends in DOC quantity and quality for all stream orders (Fig. 5), suggesting that on average DOC cycling at the SGI is consistent and does not correlate with stream order. Additionally, the 7 sites that showed clear removal of DOC at the

SGI vary in stream order and location in the watershed (Table 1), further suggesting that DOC transformations at the SGI occur independent of stream order and are controlled by more local scale hydrologic and biogeochemical conditions. Finally, the metabolism plot that accounts for VHG (Fig. 8c), showed no pattern of DOC utilization based on VHG, suggesting that DOC cycling at the SGI may not correlate with changes in local hydrologic flow direction, but this is based on a very limited number of sites (n=4) and more observations are needed to assess this relationship.

The lack of a relationship observed between DOC transformations in the SGI and stream order as well as VHG may be complicated by numerous factors. Variations in land use/cover (see Supplemental Information, Fig. S1) may influence trends in DOC quantity and quality at the SGI at the sub-network scale, and therefore, should be consider when comparing trends between sites across the network. Additionally, lateral flowpaths that intersect our vertical profiles further complicate interpretations of processes driving trends in DOC quantity and quality. Using Cl^- concentrations as a natural tracer enabled us to separate sites influenced by lateral flowpaths from sites exhibiting 1D vertical mixing. Further, the Cl^- concentrations allowed us to remove the changes in DOC concentrations due to vertical mixing, which allowed for more accurate assessment of the DOC mass removed at the SGI and the associate removal processes. However, future studies are needed that improve characterization of the end-member waters, potentially via coupled tracer studies, in order to enhance understanding of the SGI flow field at each site. Lastly, we observed only 7 sites that clearly showed evidence of DOC removal at the SGI. This might have been due to the increase in stage height across the network that resulted from two precipitation events that occurred during the sampling campaign (Fig. 2). An increase in stage height will cause a change in the flux of water and DOC through the SGI. The specific effect on

591 the SGI flow field, including VHG changes, at each site under the elevated stream flows is not
592 known. If, for example, the storm increased the groundwater discharge to the stream, we can
593 expect that VHG would increase, while residence times of water and solutes in the SGI would
594 decrease, which, in turn, is likely to decrease DOC processing and uptake in the SGI (Zarnetske
595 et al. 2012). As seen in the VHG data, Augusta Creek is clearly a groundwater gaining stream in
596 most locations, and the storm event likely altered the groundwater discharge conditions at many
597 of our sampling sites. Therefore, we predict that sampling under low to baseflow conditions at
598 Augusta Creek, would yield different SGI DOC patterns. Consequently, despite the significant
599 effort to conduct these synoptic, network-wide, sampling campaigns, it is still recommended that
600 sites be revisited under multiple seasonal and stream flow conditions. It is also possible that
601 predicted changes in processes in the SGI across the watershed might better follow the River
602 Continuum Concept had the storm event not altered baseflow conditions.

603 Overall, these findings reveal the extreme complexities that occur in lowland watersheds
604 where groundwater discharge interacts with hyporheic exchange at the SGI, especially when
605 studies are attempted at the network scale. The complexity observed in this study brings into
606 question our ability to link and leverage surface water based conceptual models for DOC
607 biogeochemistry (e.g., River Continuum Concept and Shunt-Pulse Concept) to the SGI DOC
608 biogeochemistry. Further, the observed complexity brings into doubt the applicability and
609 accuracy of physically based models to predict SGI exchange and biogeochemistry, especially at
610 the network scale (e.g., Kiel and Cardenas 2014; Gomez-Velez and Harvey 2014), because they
611 are more typically parameterized for steeper, upland river systems where SGI exchange is
612 controlled more by surface channel morphology (Ward et al. 2013) and less so by regional
613 groundwater discharge.

Conclusions

We used synoptic sampling of the SGI across a third-order, lowland stream network to explore DOC cycling at the network (i.e., watershed) scale. Specifically, we were interested in addressing the following research questions: 1) is there evidence of DOC removal at the SGI across the stream network, 2) what processes (i.e., abiotic or biotic) are influencing DOC concentrations at the SGI, and 3) how consistent is the evidence for removal and types of processes occurring at the SGI across the network? Our findings indicate that there is no clear pattern of DOC removal at the SGI across the stream network. The trends in DOC quantity and quality suggest that the system is more complex with local site controls dominating DOC patterns in the SGI. While a small fraction of the sampling sites showed evidence of DOC removal at the SGI, hydrological processes such as lateral flowpaths and mechanical mixing controlled most of the changes in DOC at the majority of sites. In terms of the mechanism(s) driving DOC transformations at the SGI, the metabolism plots are consistent with our hypothesis that aerobic microbial respiration was predominantly consuming DOC at the SGI. Additionally, the role of the SGI as a processor of stream DOC in this lowland, groundwater-dominated watershed does not appear to be related with stream order or local hydrologic flow patterns (i.e., upwelling versus downwelling sites).

This work represents one of the first ever attempts to measure SGI biogeochemistry at the network scale, and it reveals that if a biogeochemical process is a key research objective, you need to collect significant complementary hydrological (e.g., VHG) and chemical (conservative ion tracer) data in order to isolate the mechanisms controlling the fate of DOC in the SGI. Consequently, we suggest a systematic approach for sampling DOC at the SGI at the network

637 scale (i.e., “lessons learned”). We also see that additional studies are needed to more fully assess
638 the main objective of determining if the SGI functions as a net sink of DOC in the watershed,
639 and if this DOC removal is primarily controlled by biological processing. This is not to say that
640 the SGI of other stream networks, especially those that are of more upland, steeper streams, will
641 not have more clear DOC removal patterns at local and networks scales as indicated by previous
642 smaller-scale studies (e.g., Baker et al. 1999; Fischer et al. 2005; Battin et al. 2009; Zarnetske et
643 al. 2011b). However, for less frequently studied lowland streams, these biogeochemical patterns
644 are likely confounded by the influence of upwelling groundwater. Thus, for this lowland study
645 stream, further work includes conducting similar synoptic field studies that 1) are at baseflow
646 conditions, to eliminate the complexity introduced by storm events and 2) more accurately
647 characterize the end-member waters (potentially via coupled tracer studies), in order to improve
648 understanding of the hydrology at each site. By doing so, it would expand the number of sites
649 across the stream network where researchers could interpret the trends in DOC quantity and
650 quality, which is needed to answer questions about processes driving DOC cycling at the SGI at
651 site or network scales.
652

653 **Acknowledgements**

654 The authors would like to thank Stephen K. Hamilton, Dustin Kincaid, Tudor Big, and Tyler
655 Hampton for their valuable contributions, discussions, and field assistance. Support for this
656 research was partially provided by a Geological Society of America Graduate Student Research
657 Grant as well as by the NSF Long-term Ecological Research Program (DEB 1027253) at the
658 Kellogg Biological Station and by Michigan State University AgBioResearch.
659

660 **Supplemental Information**

661 Provided as supplemental materials are the vertical porewater profiles for DOC concentration
662 (observed and predicted), DOC quality indices, dissolved oxygen, temperature, and various ions
663 for all 39 individual sites sampled during the 2016 synoptic sampling campaign. Also included
664 are the land use/cover types present across the watershed and the integration method for the
665 metabolism plot in Fig. 8b, c.

666

667 **References**

668 Baker MA, Dahm CN, Valett HM (1999) Acetate retention and metabolism in the hyporheic
669 zone of a mountain stream. Limnol Oceanogr 44:1530-1539. doi:
670 10.4319/lo.1999.44.6.1530.

671 Battin TJ (1999) Hydrologic flow paths control dissolved organic carbon fluxes and metabolism
672 in an alpine stream hyporheic zone. Water Resour Res 35:3159-3169. doi:
673 10.1029/1999WR900144.

674 Battin TJ, Kaplan LA, Findlay S, Hopkinson CS, Marti E, Packman AI, Newbold JD, Sabater F
675 (2008) Biophysical controls on organic carbon fluxes in fluvial networks. Nat Geosci
676 1:95–100. doi: 10.1038/ngeo101.

677 Battin TJ, Luyssaert S, Kaplan LA, Aufdenkampe AK, Richter A, Tranvik LJ (2009) The
678 boundless carbon cycle. Nat Geosci 2:598–600. doi: 10.1038/ngeo618.

679 Boano F, Harvey JW, Marion A, Packman AI, Revelli R, Ridolfi L, Wörman A (2014)
680 Hyporheic flow and transport processes: Mechanisms, models, and biogeochemical
681 implications. Rev Geophys 52:603-679. doi: 10.1002/2012RG000417.

682 Cory RM, Boyer EW, McKnight DM (2011) Spectral methods to advance understanding of
683 dissolved organic carbon dynamics in forested catchments. Forest Hydrology and

684 Biogeochemistry: Synthesis of past Research and Future Directions 117–135. doi:
685 10.1007/978-94-007-1363-5.
686 Creed et al. (2015) The river as a chemostat: fresh perspectives on dissolved organic matter
687 flowing down the river continuum. J Fish Aquat Sci 72:1272–1285. doi: 10.1139/cjfas-
688 2014-0400.
689 Dahm CN (1981) Pathways and mechanism for removal of dissolved organic carbon from leaf
690 and leachate in streams. Can J Fish Aquat Sci 38:68-76. doi: 10.1139/f81-009.
691 Day GM, Hart BT, McKelvie ID, Beckett R (1994) Adsorption of natural organic matter onto
692 goethite. Colloid Surface A 89:1-13. doi: 10.1016/0927-7757(94)02855-9.
693 Dunbar CO (1962). Historical Geology. 2nd edn. John Wiley and Sons, New York, pp 500.
694 Duff JH, Murphy F, Fuller CC, Triska FJ, Harvey JW, Jackman AP (1998) A mini drivepoint
695 sampler for measuring pore-water solute concentrations in the hyporheic zone of sand-
696 bottom streams. Limnol Oceanogr 43:1378–1383. doi: 10.4319/lo.1998.43.6.1378.
697 Fellman JB, Hood E, Spencer RGM (2010) Fluorescence spectroscopy opens new windows into
698 dissolved organic matter dynamics in freshwater ecosystems: a review. Limnol Oceanogr
699 55:2452–2462. doi: 10.4319/lo.2010.55.6.2452.
700 Fiebig DM, Lock MA (1991) Immobilization of dissolved organic matter from groundwater
701 discharging through stream bed. Freshwater Biol 26:45-55. doi: 10.1111/j.1365-
702 2427.1991.tb00507.x.
703 Fiebig DM (1995) Groundwater discharge and its contribution of dissolved organic carbon to an
704 upland stream. Archiv Für Hydrobiologie 134:129-155.

705 Findlay S, Strayer D, Goumbala C, Gould K (1993). Metabolism of streamwater dissolved
706 organic carbon in the shallow hyporheic zone. Limnol Oceanogr 38:1493-1499. doi:
707 10.4319/lo.1993.38.7.1493.
708 Findlay S, Sobczak WV (1996) Variability in removal of dissolved organic carbon in hyporheic
709 sediments. J North Am Benthol Soc 15:35–41. doi: 10.2307/1467431.
710 Findlay S, Sobczak WV (2000) Microbial communities in hyporheic sediments. In Jones JA and
711 Mulholland PJ (ed) Streams and Ground Waters, Academic Press, California, pp 287-
712 306.
713 Fischer H, Kloep F, Wilzcek F, Pusch MT (2005) A river's liver – microbial processes within the
714 hyporheic zone of a large lowland river. Biogeochem 76:349-371. doi: 10.1007/s10533-
715 005-6896-y.
716 FTWRC, Four Townships Water Resources Council (2011) Gull and Augusta Creeks Watershed
717 Management Plan: the Four Township Watershed Area. Accessed from
718 http://www.ftwrc.org/publications/FTWA_WMP_final.pdf.
719 Gomez-Velez JD, Harvey JW (2014) A hydrogeomorphic river network model predicts where
720 and why hyporheic exchange is important in large basins. Geophys Res Lett 41:6403-
721 6412. doi: 10.1002/2014GL061099.
722 Harvey JW, Fuller CC (1998) Effect of enhanced manganese oxidation in the hyporheic zone on
723 basin-scale geochemical mass balance. Water Resour Res 34:623-636. doi:
724 10.1029/97WR03606.
725 Harvey JW, Böhlke JK, Voytek MA, Scott D, Tobias CR (2013) Hyporheic zone denitrification:
726 Controls on effective reaction depth and contribution to whole-stream mass balance.
727 Water Resour Res 49:6298-6316. doi: 10.1002/wrcr.20492.

728 Hedin LO, von Fischer JC, Ostrom NE, Kennedy BP, Brown MG, Robertson GP (1998)
729 Thermodynamic constraints on nitrogen transformations and other biogeochemical
730 processes at soil-stream interfaces. Ecology 79:684-703. doi: 10.2307/176963.
731 Helms JR, Stubbins A, Ritchie JD, Minor EC (2008) Absorption spectral slopes and slope ratios
732 as indicators of molecular weight, source, and photobleaching of chromophoric dissolved
733 organic matter. Limnol Oceanogr 53:955–969. doi: 10.4319/lo.2008.53.3.0955.
734 Helton AM, Wright MS, Bernhardt ES, Poole GC, Cory RM, Stanford JA (2015) Dissolved
735 organic carbon lability increases with water residence time in the alluvial aquifer of a
736 river-floodplain ecosystem. J Geophys Res-Biogeo 120:693-706. doi:
737 10.1002/2014JG002832.
738 Jamieson R, Joy DM, Lee H, Kostaschuk R, Gordon R (2005) Transport and deposition of
739 sediment-associated *Escherichia coli* in natural stream. Water Res 39:2665-2675. doi:
740 10.1016/j.watres.2005.04.040
741 Jollymore A, Johnson MS, Hawthorne I (2012) Submersible UV–Vis spectroscopy for
742 quantifying streamwater organic carbon dynamics: implementation and challenges before
743 and after forest harvest in a headwater stream. Sensors 12:3798–3813. doi:
744 10.3390/s120403798.
745 Kaplan LA, Newbold JD (2000) Surface and subsurface dissolved organic carbon, in Jones JA
746 and Mulholland JP (ed) Streams and Ground Waters, Academic Press, California, pp
747 237-258.
748 KBS-LTER, Dataset KBS002. Annual Temperature and Precipitation, Data Table KBS002-
749 008.61. Accessed on 7 Mar 2017. Permission to use data granted from lead investigator,
750 Phil Robertson.

751 Kiel BA, Cardenas MB (2014) Lateral hyporheic exchange throughout the Mississippi River
752 network. Nat Geo 7:413-417. doi: 10.1038/ngeo2157.
753 King RH (1978) Natural history and ecology of the stictochironomous annulicrus (townes)
754 (diptera:chrionomidae), Augusta Creek, Kalamazoo County, Michigan. Dissertation.
755 Michigan State University.
756 Lutz BD, Bernhardt ES, Roberts BJ, Cory RM, Mulholland PJ (2012) Distinguishing dynamics
757 of dissolved organic matter components in a forested stream using kinetic enrichments.
758 Limnol Oceanogr 57:76-89. doi: 10.4319/lo.2012.57.1.0076.
759 Mann PJ, Davydova A, Zimov N, Spencer RGM, Davydov S, Bulygina E, Zimov S, Holmes RM
760 (2012) Controls on the composition and lability of dissolved organic matter in Siberia's
761 Kolyma River basin. J Geophys Res-Biogeo 117:1–15. doi: 10.1029/2011JG001798
762 Manny BA, Wetzel RG (1973) Diurnal changes in dissolved organic and inorganic carbon and
763 nitrogen in a hardwater stream. Freshw Biol 3:31–43. doi: 10.1111/j.1365-
764 2427.1973.tb00060.x.
765 Mahan DC, Cummins KW (1974) A profile of Augusta Creek in Kalamazoo and Barry Counties,
766 Michigan. Tech Rep No. 3. W.K. Kellogg Biological Station, Michigan State University.
767 Marshall KC (1980) Adsorption of microorganisms to soils and sediments. In Bitton G and
768 Marshall KC (ed) Adsorption of Microorganisms to Surfaces, Wiley, New York, pp 317-
769 330.
770 McDowell WH (1985) Kinetics and mechanisms of dissolved organic carbon retention in a
771 headwater stream. Biogeochem 4:329-352. doi: 10.1007/BF02187376.
772 McKnight DM, Boyer EW, Westerhoff PK, Doran PT, Kulbe T, Andersen DT (2001)
773 Spectrofluorometric characterization of dissolved organic matter for indication of

precursor organic material and aromaticity. Limnol Oceanogr 46:38–48. doi: 10.4319/lo.2001.46.1.0038.

NCDC, National Climate Data Center (2013). Summary of Monthly Normal 1981-2010. Gull Lake Biology Station, Michigan, USA. Accessed January 17, 2013 at http://www.ncdc.noaa.gov/cdo-web/search.

Nogaro G, Datry T, Mermillod-Blondin F, Foulquier A, Montuelle B (2013) Influence of hyporheic zone characteristics on the structure and activity of microbial assemblages. Freshw Biol 58:2567-2583. doi: 10.1111/fwb.12233.

Peters NE, Ratcliffe EB (1998) Tracing Hydrologic Pathways Using Chloride at the Panola Mountain Research Watershed, Georgia, USA. Water, Air, and Soil Pollution 105:263-275. doi: 10.1023/A:1005082332332.

Pinder GF, Jones JF (1969) Determination of the ground-water component of peak discharge from the chemistry of total runoff. Water Resour Res 5:438-445. doi: 10.1029/WR005i002p00438.

Poff NL, Allan JD, Bain MB, Karr JR, Prestegaard KL, Richter BD, Sparks RE, Stromberg JC (1997) The Natural Flow Regime: A paradigm for river conservation and restoration. Bioscience 47:69–784. doi:10.2307/1313099.

Potter B, Wimsatt J (2003) US EPA Method 415.3 –Determination of TOC and SUVA at 254nm in Source Water and Drinking Water. National Exposure Research Laboratory, Office of Research and Development, US EPA, Cincinnati, Ohio.

Raymond PA, Saiers JE, Sobczak WV (2016) Hydrological and biogeochemical controls on watershed dissolved organic matter transport: pulse-shunt concept. Ecology 97:5-16. doi: 10.1890/14-1684.1.

797 Ruhala SS, Zarnetske JP (2017) Using in-situ optical sensors to study dissolved organic carbon
798 dynamics of streams and watersheds: A review. Sci Total Environ 575:713-723. doi:
799 10.1016/j.scitotenv.2016.09.113.
800 Schindler JE, Krabbenhoft DP (1998) The hyporheic zone as a source of dissolved organic
801 carbon and carbon gases to a temperate forested stream. Biogeochem 43:157-174. doi:
802 10.1023/A:1006005311257.
803 Sobczak WV, Findlay S (2002) Variation in bioavailability of dissolved organic carbon among
804 stream hyporheic flowpaths. Ecology 83:3194–3209. doi: 10.2307/3071853.
805 Stelzer RS, Scott JT, Bartsch LA (2015) Buried particulate organic carbon stimulates
806 denitrification and nitrate retention in stream sediments at the groundwater-surface water
807 interface. Freshw Sci 34:161-171. doi:10.1086/678249.
808 Storey RG, Fulthorpe RR, Williams DD (1999) Perspectives and predictions on the microbial
809 ecology of the hyporheic zone. Freshwater Biol 41:119-130. doi: 10.1046/j.1365-
810 2427.1999.00377.x.
811 Strahler AN (1957) Quantitative analysis of watershed geomorphology. Trans Amer Geophys Un
812 38:913-920.
813 USGS, United States Geological Survey (2017) National Water Information System data
814 available on the World Wide Web (USGS Water Data for the Nation). Accessed March 7,
815 2017 at https://waterdata.usgs.gov/mi/nwis/uv?site_no=04105700.
816 Url S, Hart DD (2012) International Association for Ecology Community Organization in
817 Streams: The Importance of Species Interactions. Oecologia 91:220–228. doi:
818 10.1007/BF00317787.

819 Valett HM, Morrice JA, Dahm CN (1996) Parent lithology, surface-groundwater exchange, and
820 nitrate retention in headwater streams. Limnol Oceanogr 41:333-345. doi:
821 10.4319/lo.1996.41.2.0333.
822 Vannote RL, Minshall WG, Cummins KW, Sedell JR, Cushing CE (1980) The River Continuum
823 Concept. Can J Fish Aquat Sci 37:130–137. doi: 10.1139/f80-017.
824 Ward AS, Payn RA, Gooseff MN, McGlynn BL, Bencala KE, Kelleher CA, Wondzell SM,
825 Wagener T (2013) Variations in surface water-groundwater interactions along a
826 headwater mountain stream: Comparisons between transient storage and water balance
827 analyses. Water Resour Res 49:3359-3374. doi: 10.1002/wrcr.20148.
828 Weishaar JL, Aiken GR, Bergamaschi BA, Fram MS, Fujii R, Mopper K (2003) Evaluation of
829 specific ultra-violet absorbance as an indicator of the chemical composition and reactivity
830 of dissolved organic carbon. Environ Sci Technol 37:4702–4708. doi:
831 10.1021/es030360x.
832 Wilkinson J, Jenkins A, Wyer M, Kay D (1995) Modelling faecal coliform dynamics in streams
833 and rivers. Water Res 29:847-855. doi: 10.1016/0043-1354(94)00211-O.
834 Wondzell SM (2011) The role of the hyporheic zone across stream networks. Hydrol Process
835 25:3525-3532. doi: 10.1002jhyp.8119.
836 Zarnetske JP, Haggerty R, Wondzell SM, Baker MA (2011a) Dynamics of nitrate production and
837 removal as a function of residence time in the hyporheic zone. J. Geophys. Res., 116:
838 G01025. doi:10.1029/2010JG001356.
839 Zarnetske JP, Haggerty R, Wondzell SM, Baker MA (2011b) Labile dissolved organic carbon
840 supply limits hyporheic denitrification. J Geophys Res-Biogeo 116. doi:
841 10.1029/2011JG001730.

842 Zarnetske JP, Haggerty R, Wondzell SM, Bokil V, González-Pinzón R (2012) Coupled transport
843 and reaction kinetics control the nitrate source-sink function of hyporheic zones. Water
844 Resour. Res. 48:W11508. doi:10.1029/2012WR011894.

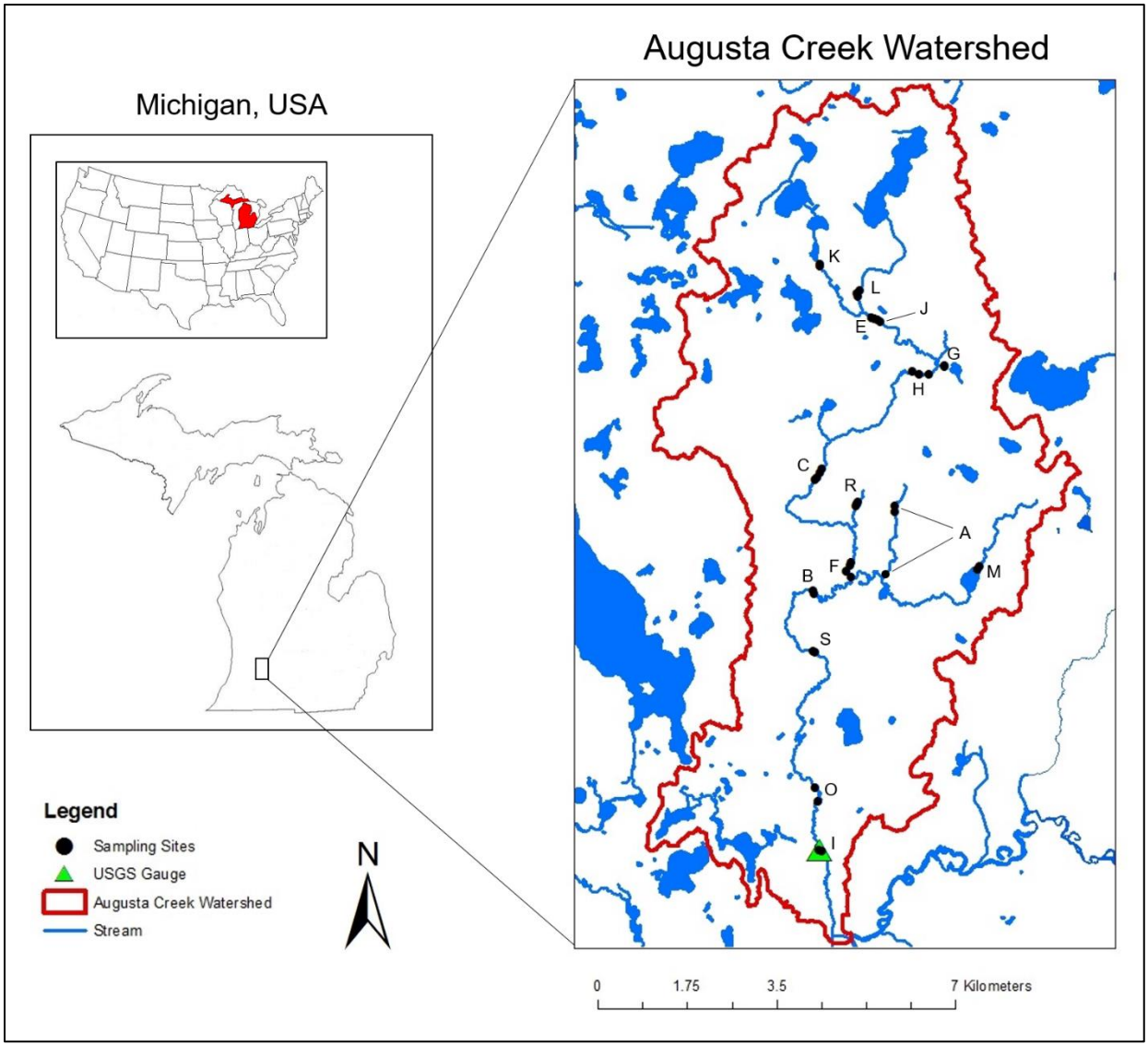

845

846 **Fig. 1** Map of the Augusta Creek watershed, Michigan, USA including the 39 sites sampled
847 during the 2016 synoptic sampling campaign. Letters refer to the sampling site groups. More
848 detailed site maps and watershed land coverages are provided in the Supplemental Information
849 (Fig. S1).

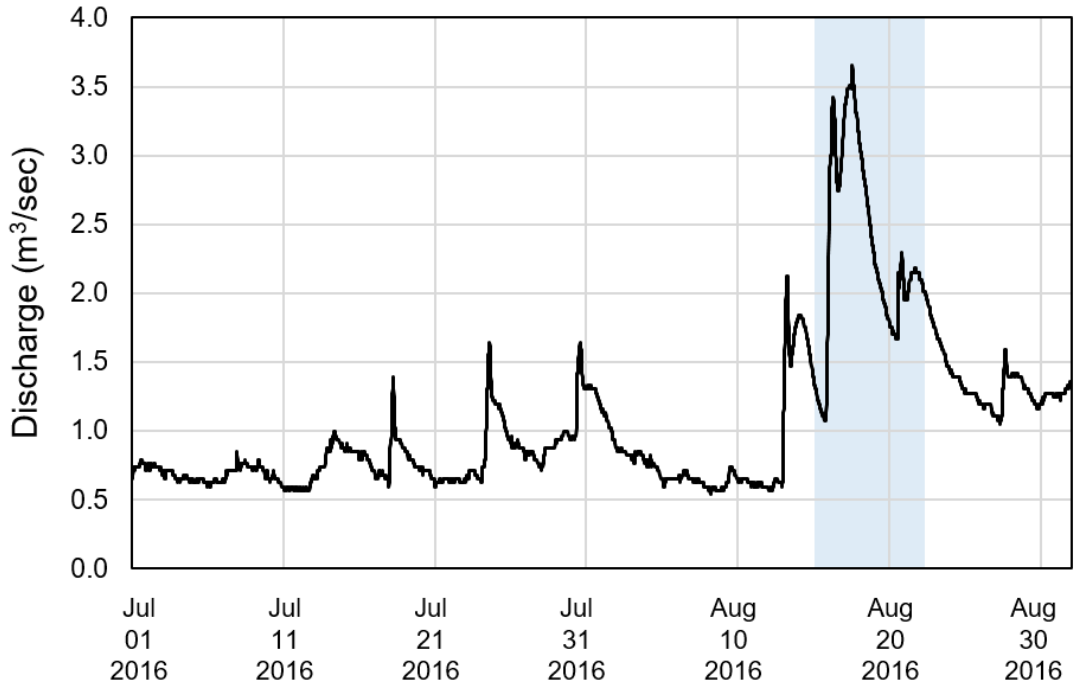

850

851 **Fig. 2** Stream discharge data from the Augusta Creek gaging station, #04105700 from July 1 –

852 September 1, 2016. The synoptic sampling campaign occurred from August 15 – August 22,

853 2016, highlighted in the blue shaded box. Data from US Geological Survey National Water

854 Information System (nwis.waterdata.usgs.gov, accessed 7 Mar 2017).

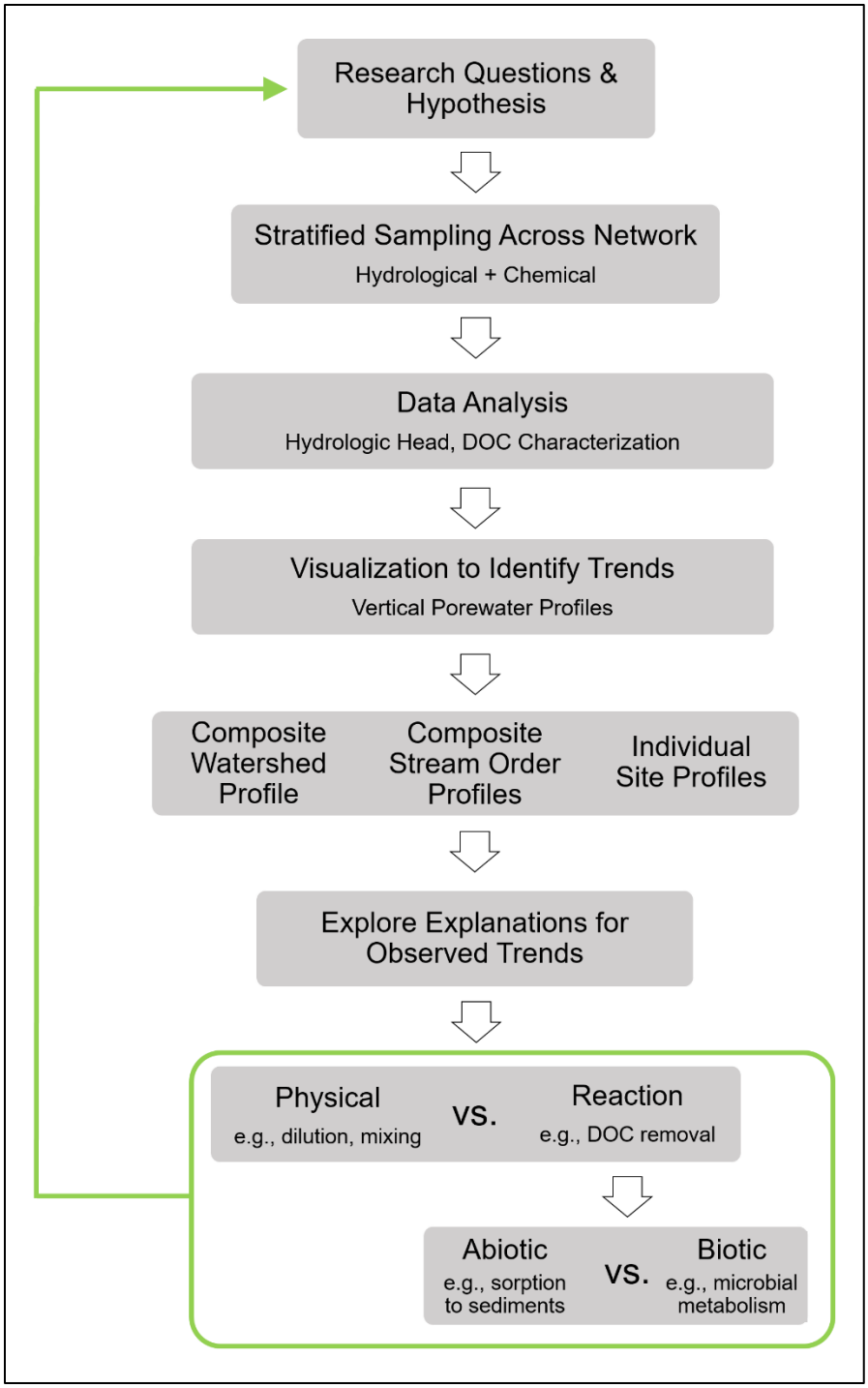

855

856 **Fig. 3** A systematic approach we developed to conduct SGI investigations at the network-scale,

857 including data analysis techniques used to assess trends in DOC quantity and quality and identify

858 potential processes driving transformations in DOC at the SGI.

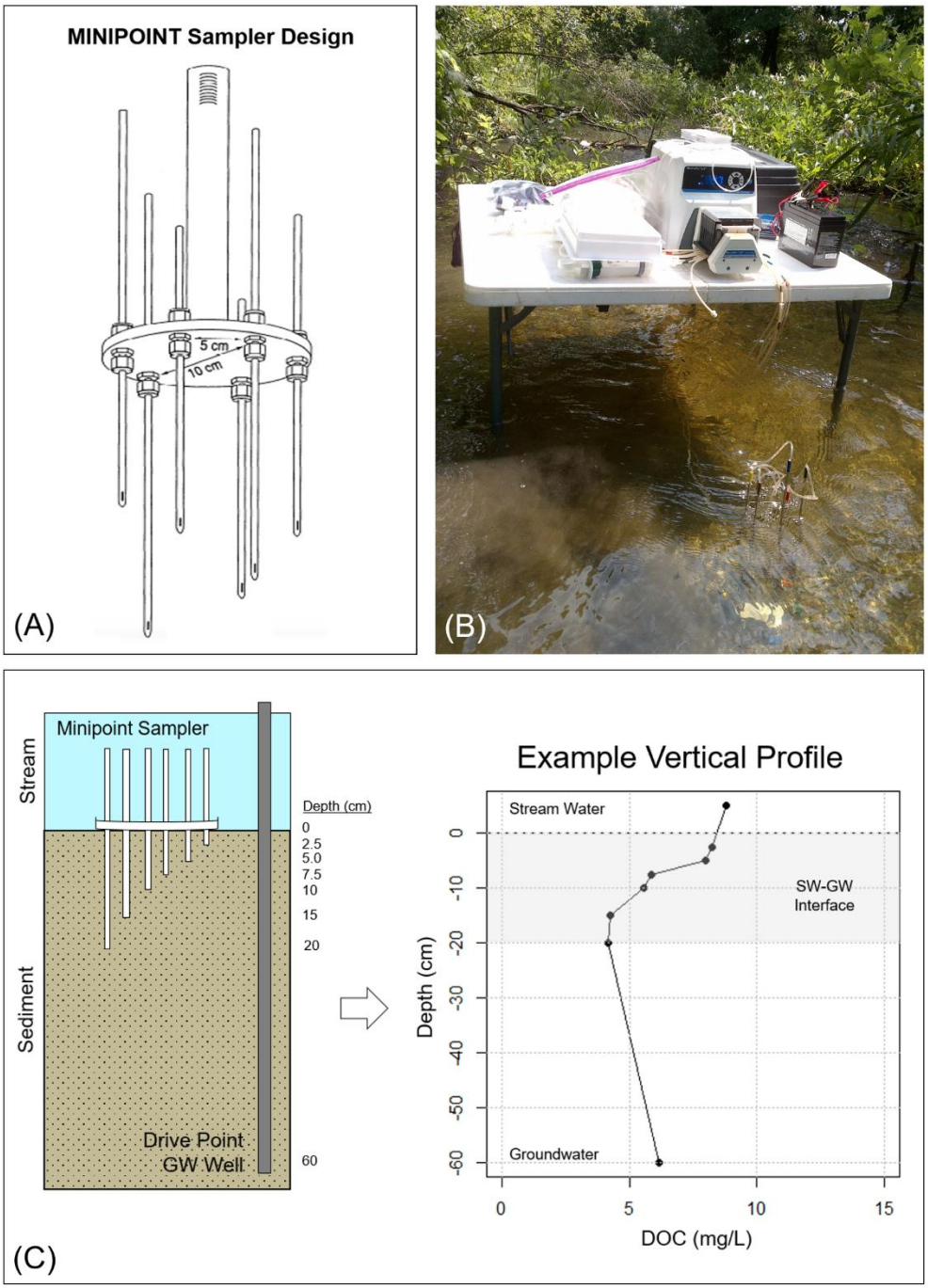

859

860 **Fig. 4** Data collection and analysis: a) the MINIPOINT sampler design (Duff et al. 1998) used
861 for SGI sampling, b) field setup used at each of the 39 sampling sites across Augusta Creek, and
862 c) an example of a vertical porewater profile used for visualization to identify trends. The
863 streambed sediment interface (i.e., 0 cm) is shown by the dashed line.

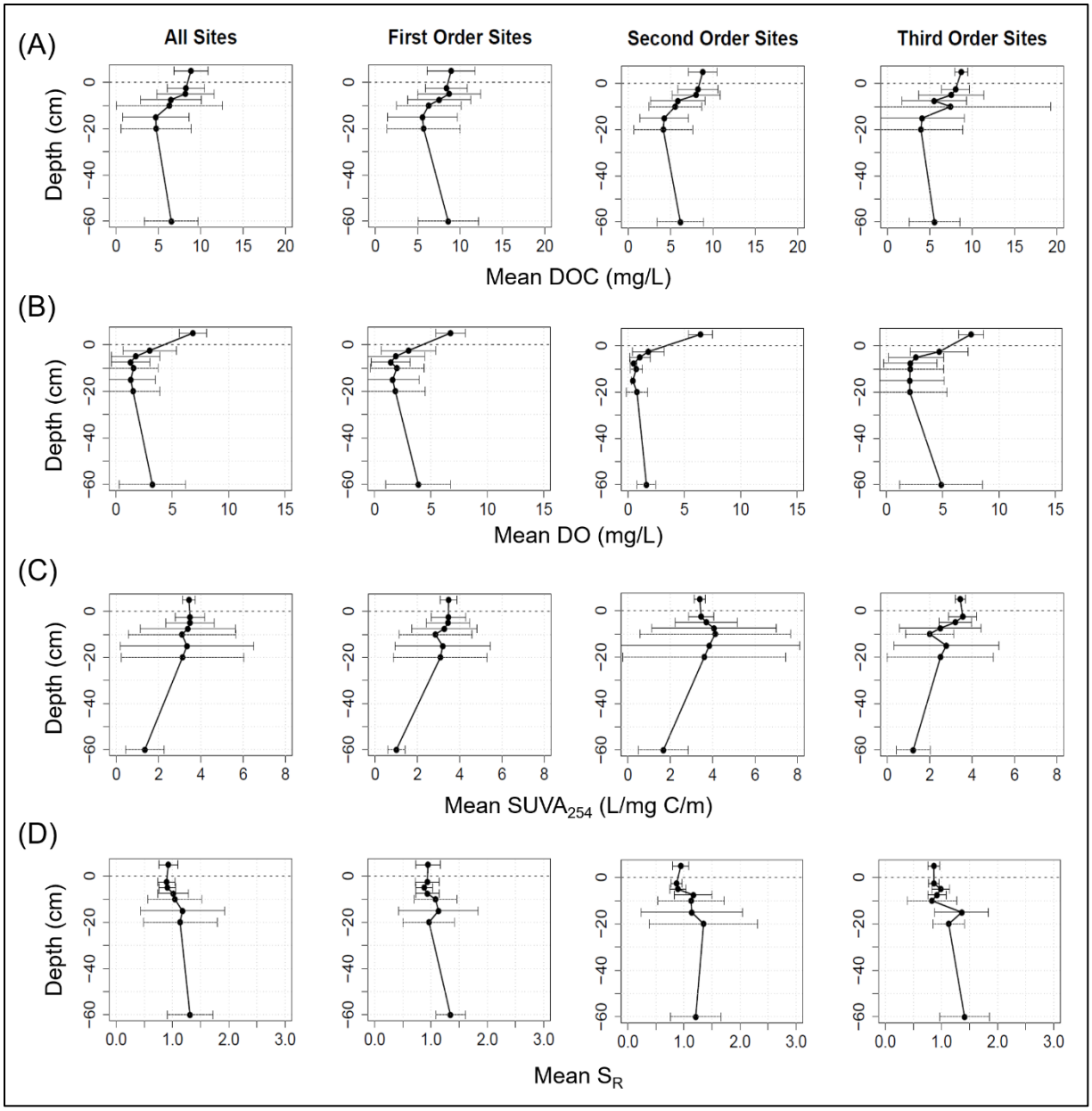

Fig. 5 Composite vertical porewater profiles of a) mean DOC, b) mean DO, c) mean $SUVA_{254}$, and d) mean S_R of all 39 sites and by stream order. Each plot includes error bars of one standard deviation; n=39 for "all sites", n=16 for "first order sites", n=14 for "second order sites" and n=9 for "third order sites."

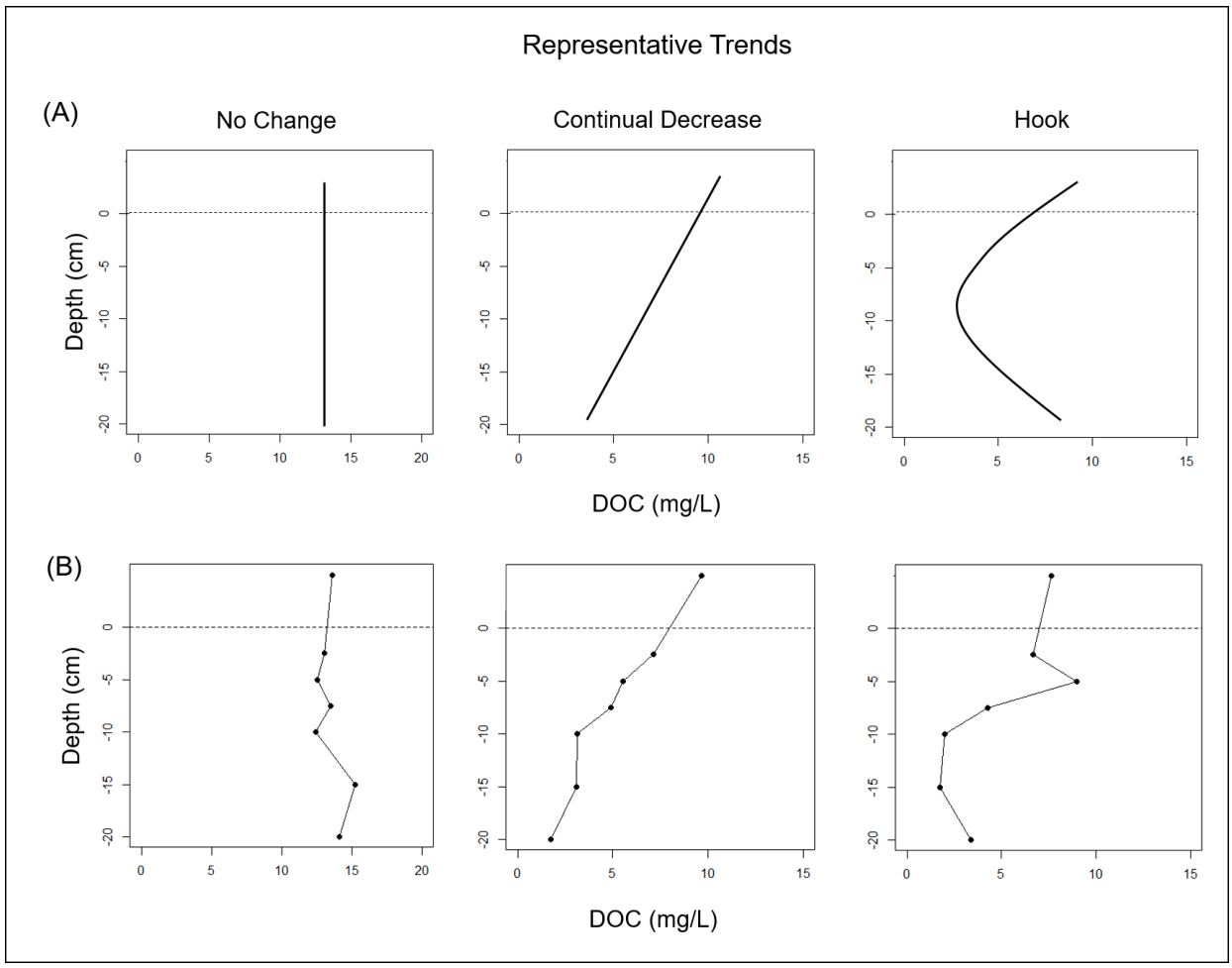

869

870 **Fig. 6** Three representative trends for the 39 individual vertical porewater profiles: a) conceptual
871 graphs for each trend with depth of SGI - no change, continual decrease, and hook. Examples
872 from Augusta Creek of each representative trend are show in b) Site L3, Site O1, Site G2 (left to
873 right).

Table 1 Summary of VHG data (D represents sites where the well was disconnected from porewater at 60 cm (i.e., dry because inserted in low permeability sediments) and N/A represents sites where VHG was not measured) and binary mixing model results. Sites in white had end-member percentages between 0 to 100%, while sites shaded in gray did not.

Site	Stream Order	VHG (+, gaining)	Process	Subtraction Approach: Range of Depth (cm)	Integration Approach: Range of Porewater Volumes (cm^3)
A1	1	0.145	Lateral Flow		
A2	1	D	Lateral Flow		
A3	1	D	Lateral Flow		
B1	3	0.066	Lateral Flow		
B2	3	0.03	Removal	2.5 – 15	0.875 – 5.25
C1	2	D	Removal	2.5 – 15	0.875 – 5.25
C2	2	0.745	Lateral Flow		
C3	2	D	Removal	2.5 – 10	0.875 – 3.5
C4	2	0.047	Lateral Flow		
E1	2	-0.655	Lateral Flow		
E2	2	-0.041	Removal	2.5 – 7.5	0.875 – 2.625
E3	2	0.381	Production		
F1	3	-0.447	Lateral Flow		
F2	2	-0.122	Lateral Flow		
F3	2	D	Lateral Flow		
F4	2	-0.117	Lateral Flow		
G1	1	N/A	Production		
G2	1	N/A	Lateral Flow		
H1	2	N/A	Lateral Flow		
H2	2	N/A	Lateral Flow		
H3	2	N/A	Production		
I1	3	0.058	Lateral Flow		
I2	3	0.038	Removal	2.5 – 15	0.875 – 5.25
J1	2	N/A	Lateral Flow		
K1	1	D	Production		
K2	1	D	Mixing		
L1	1	D	Lateral Flow		
L2	1	D	Lateral Flow		
L3	1	D	Lateral Flow		
M1	1	-1.885	Lateral Flow		
M2	1	D	Removal	2.5 – 5.0	0.875 – 1.75
O1	3	0.092	Mixing		
O2	3	0.051	N/A		
R1	1	D	Mixing		
R2	1	-0.544	Removal	2.5 – 10	0.875 – 3.5
R3	1	-0.193	Lateral Flow		
R4	1	0.152	Lateral Flow		
S1	3	0.258	Lateral Flow		
S2	3	0.667	Lateral Flow		

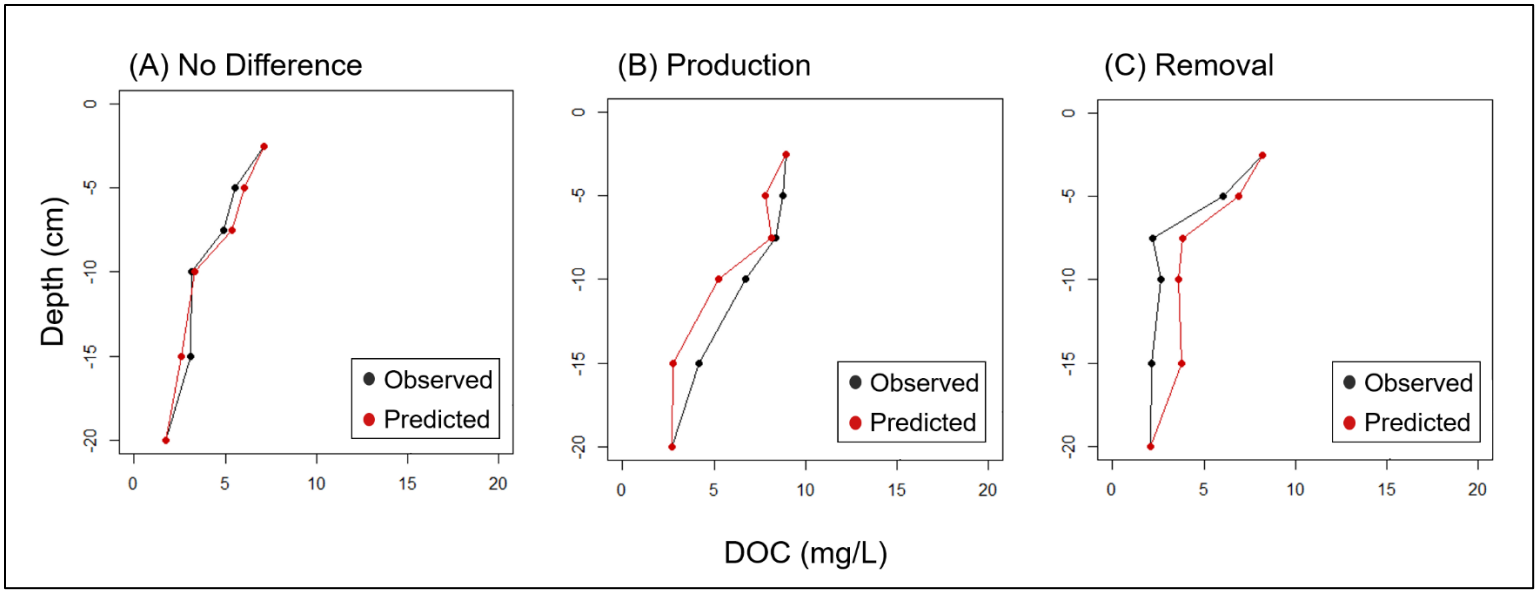

879

880 **Fig. 7** Vertical porewater profiles of observed and predicted concentrations of DOC: a) no difference between observed concentrations
881 and mixing model predicted concentrations of DOC, b) observed concentrations are greater than predicted concentrations of DOC,
882 indicating production of DOC, and c) observed concentrations are less than predicted concentrations of DOC, indicating removal of
883 DOC.

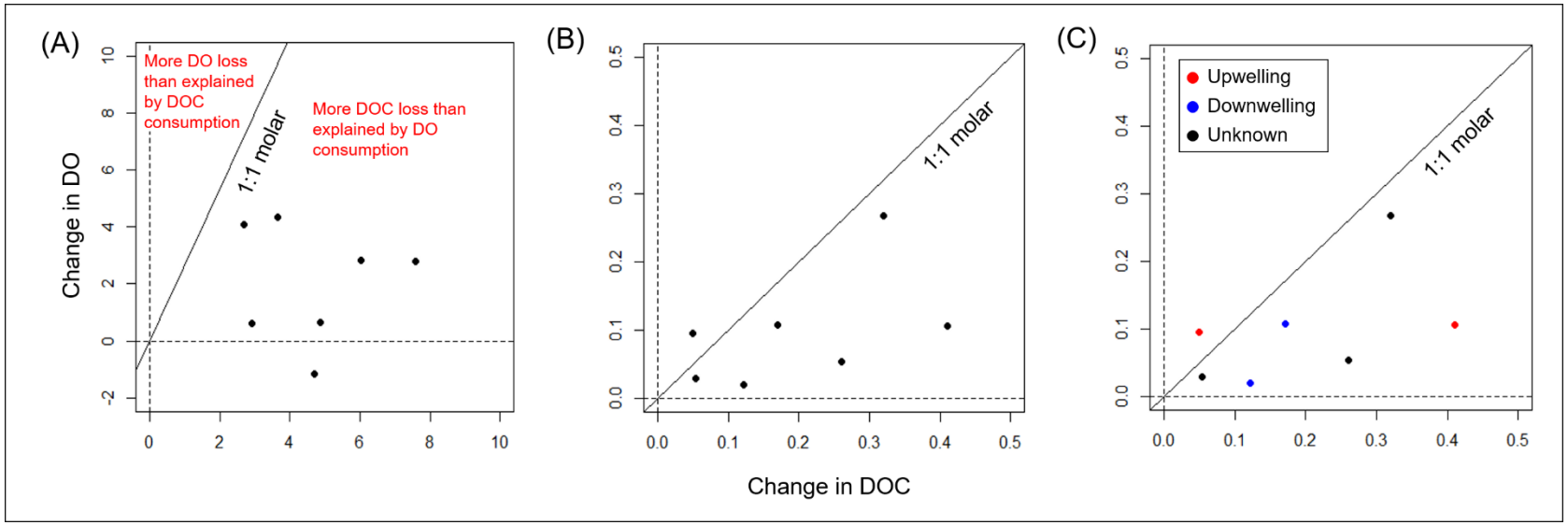

884

885 **Fig. 8** Plots of DO consumption versus DOC consumption between two given depths (i.e., metabolism plots). Metabolism plots were
886 created using the 7 sites that showed removal of DOC at the SGI: a) based on subtraction between observed DOC concentrations for a
887 selected range in SGI depth (in mg/L), b) based on integration (in µmol), and c) accounting for VHG (in µmol). If aerobic respiration
888 accounts for all DOC loss then points should fall on the 1:1 molar line, assuming that 1 mole of O_2 is consumed for every mole of
889 carbon consumed.